Different Forms of Cyclic Liquefaction Behaviours of Coal Ash

M. A. L. Baki[1], S.M. ASCE; M. M. Rahman[2], A.M. ASCE and S. R. Lo[3]

[1]School of Engineering and Information Technology (SEIT), University of New South Wales (UNSW), Canberra, ACT 2600; PH (+612) 626 88338; FAX (+612) 626 88337; email: engbakiruet@yahoo.com
[2]Lecturer, School of Natural and Built Environments, University of South Australia, Mawson Lakes, Adelaide, South Australia 5001; PH (+618) 830 25899; FAX (+618) 830 25082; email: Mizanur.Rahman@unisa.edu.au
[3]Associate Professor, SEIT, UNSW, Canberra, ACT 2600; PH (+612) 626 88349; FAX (+612) 626 88337; email: r.lo@adfa.edu.au

ABSTRACT

Although research advancement has been made in understanding different forms of cyclic liquefaction behaviours of clean as well as silty sands, it is not well understood for coal ash which is predominantly fines (particles smaller than 0.075 mm in diameter). Previous investigations on cyclic liquefaction of coal ash were largely cyclic mobility studies without examining the form of cyclic liquefaction. Thus, the present study is directed to investigate and categorise different forms of cyclic liquefaction behaviours of coal ash. Both one-way (in compression) and two-way symmetrical cyclic loading were covered by the testing program.

Keywords: coal ash, cyclic instability, cyclic mobility, fines.

1 INTRODUCTION

Coal ash is a coal combustion by-products largely generated from coal-fire based electric power plants and contains significant amount of fines. Due to the higher transportation cost to place in a construrction site, coal ash is generally disposed in large ash ponds by pumping in saturated state. The susceptibility of such saturated fill material against liquefaction potential has been a great concern to the geotechnical engineers (Boominathan and Hari 2002; Jakka et al. 2010).

Liquefaction can be divided into either static or cyclic depending on whether the loading trigger is monotonic or cyclic. Cyclic liquefaction can occur in the form of either cyclic instability or cyclic mobility (Baki et al. 2011). Cyclic instability (Mohamad and Dobry 1986; Baki et al. 2011) is a deviatoric strain softening behaviour triggered by a series of cyclic stress pulses. For this type of liquefaction, instability in the context of continuum mechanics, i.e. $d\sigma_{ij}d\varepsilon_{ij} < 0$ (Lade 1994), is manifested, where σ_{ij} and ε_{ij} are stress and strain tensors respectively and "d" represents infinitesimal increments. Cyclic mobility (Ishihara 1993) can be categorised as a state of occurrence of 5% double amplitude (DA) axial strain and the effective stress path (ESP) travels transiently to near zero in a load cycle, but the prescribed peak and trough deviator stress (q_{peak} and q_{trough} respectively) can still be developed even a few loading cycles after the occurrence of cyclic mobility. Figure 1 shows typical cyclic instability and cyclic mobility behaviour.

A limited number of studies have been found in literature that directly investigated cyclic liquefaction behaviour of coal ash under triaxial testing. Among those limited studies, test results were interpreted along the lines of cyclic mobility studies. For example, Zand et al. (2009) showed that, at a constant effective mean stress (prior to shearing), p'_0 and a given cyclic stress ratio (CSR), number of loading cycles required to cause liquefaction increased with increase in relative densities. Mohanty et al. (2010) reported similar results for pond ash tested at a constant p'_0 and under one-way cyclic loading. But, it is of note that Zand et al. (2009) defined liquefaction as a state of effective confining stress reduced to near-zero as a results of cyclic loading and followed by a dramatic increase in axial deformation, whereas Mohanty et al. (2010) considered number of loading cycles required to cause 5% total axial strain as a measure of soil failure. Also, in those two studies, no cyclic ESP and/or deviator stress-strain (q-ε_q) response was reported that could lead to categorise forms of cyclic liquefaction in either cyclic instability or cyclic mobility. On the other hand, for a given CSR and density, Jakka et al. (2010) showed that number of loading cycles required to cause liquefaction of Badarpur pond ash increased with decrease in p'_0 by using the same definition of liquefaction as used by Zand et al. (2009). Furthermore, although manifested cyclic liquefaction behaviour were different as

recognised from presented ESP and q-ε_q responses of two cyclic tests, Jakka et al. (2010) used same criteria to define liquefaction and to synthesise test results. From the above discussion, the need of categorisation and defining different forms of cyclic liquefaction behaviour of coal ash is revealed. The objective of this study is to investigate and categorise different forms of cyclic liquefaction of coal ash covering both one-way (compression) and two-way symmetrical cyclic loading.

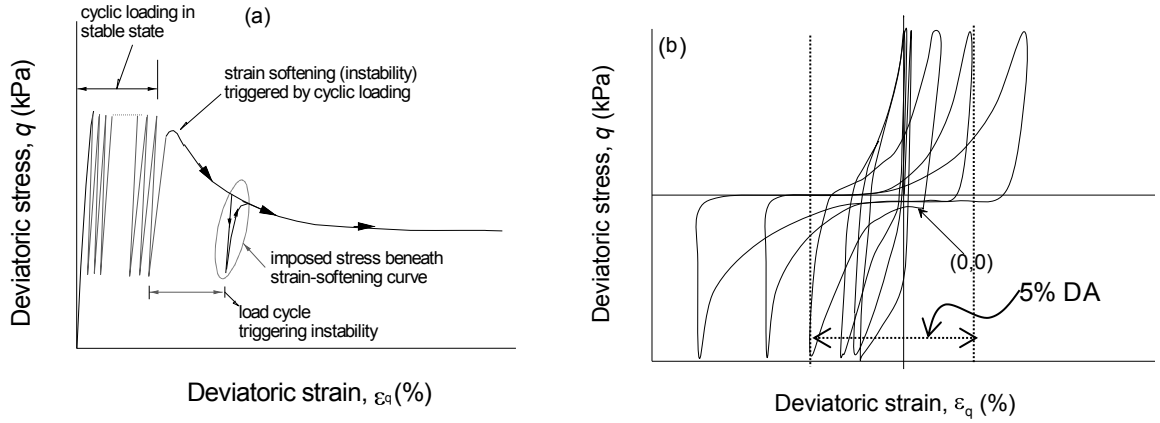

Figure 1. Typical deviator stress–strain (q-ε_q) response showing (a) triggering of cyclic instability under one-way cyclic loading and (b) cyclic mobility under two-way symmetrical cyclic loading

2 TESTED MATERIALS AND EXPERIMENTAL PROCEDURE

Coal ash sourced from a coal power station in Queensland, Australia, was used in this study as a test material. It contained 68% non-plastic fines by dry weight. Specific gravity, mean particle size and uniformity coefficient of the tested coal as was 2.04, 0.034 mm and 5.2 respectively. Grading curve of tested material is shown in Figure 2. Scanning electron microscope (SEM) images and percentages of different oxide composition (as determined from X-Ray Fluorescence (XRF) analysis) of tested coal ash can be found in Baki et al. (2012).

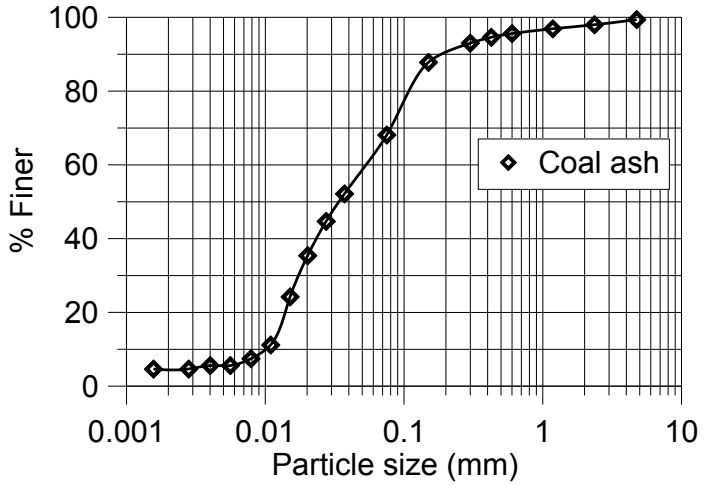

Figure 2. Grain size distribution of tested coal ash

For this study, a triaxial testing system with PC-controlled data logging and stress/strain control capabilities was used. Cyclic loadings were applied in a stress-controlled mode, but with continuous corrections by the control software to allow for change in cross-section area. The force actuator used to apply force was driven by a geared stepper motor, which was not a fast response system. This means when the actuator attempts to apply force exceeding the resistance of the specimen, it will not lead to catastrophic runoff deformation even if the specimen was brought to a state of instability. This attribute, plus having the force actuator located in line of loading train that had a mass of approximately 30 kg, also damped down acceleration during failure. Therefore, during strain softening (instability) under cyclic loading, the maximum deviator stress, q_{max} that could be mobilised (as

measured by an internal load cell) would be less than q_{peak}; and a strain softening response might also be detected under stress-controlled testing (Vaid and Sivathayalan 2000; Lo et al. 2010).

Cylindrical soil specimens of 100 mm diameter X 100 mm height were prepared by moist tamping in 10 layers at 30% moisture content. By controlling the weight and tamped thickness of each layer, the as-placed void ratio was strictly controlled. End restraint was minimized using enlarged end platen with free ends technique as described in Lo et al. (1989). All specimens were saturated to ensure B-values ≥ 0.98. The frequency of load cycle varied from 1200 to 1800 sec/cycle depending on the q_{peak} and q_{trough}.

3 TESTING PROGRAM

The testing program for this investigation comprises a total of 10 undrained cyclic triaxial tests performed under one-way and two-way (symmetrical) cyclic loading. The covered range of p'_0 varied from 100 to 850 kPa. Table 1 summarises the details of the tests conducted for this study. Due to page length limitation, 3 representative tests are included for discussion in the following section.

Table 1: Summary of cyclic tests conducted for this study

Test ID	p'_0 (kPa)[a]	Void ratio, e_0[a]	Observed behaviour
BC1-15	350	1.03	Cyclic instability
BC1-04	600	0.96	
BC1-14	850	1.00	
BC2-12	100	1.08	
BC2-02	350	0.99	
BC2-10	350	1.04	
BC2-03	600	1.00	
BC2-19	350	0.85	Cyclic mobility
BC2-07	600	0.82	
BC2-08	850	0.81	

[a] Prior to shearing

4 DISCUSSION ON TEST RESULTS

4.1 Cyclic instability

4.1.1 Cyclic instability under one-way cyclic loading in compression

Test BC1-14 commenced under p'_0 = 850 kPa with e_0 = 1.00. The ESP and q-ε_q response of this test are presented in Figures 3 a-b and the time traces of q, excess pore water pressure (pwp) and ε_q for the few cycles before and after cyclic instability are in Figure 3 c. It is to be noted that "dotted lines" in the time–trace plots indicates the occurrence (time) of q_{peak}.

For BC1-14, three stages of cyclic loadings with different q_{peak} were imposed after brought to a q of 184 kPa. In the first packet of cyclic loading, q_{peak} was 240 kPa and continued for only 5 loading cycles as the leftward movement of the cyclic ESP was getting very slow after first loading cycle. This was due to q_{peak} which was not enough magnitude to accelerate pwp development and hence leftward movement of cyclic ESP. In the second stage of cyclic loading, q_{peak} was increased to 363 kPa. As a result, the progress of the cyclic ESP towards the left initially increased but then reduced as the load cycle progressed. Thus, after 19 cycles in second stage, the third stage of cyclic loading with q_{peak} of 435 kPa was imposed. Therefore, excess pwp development per loading cycle became faster than before (Figure 3 c) and caused the cyclic ESP to move left with a accelerated rate than before (Figure 3 a). The development of ε_q accelerated suddenly from point "A" (Figure 3 b). At "A", cyclic instability triggered because the condition $dq\, d\varepsilon_q < 0$ manifested as q was reducing with increase in ε_q in loading direction (Figure 3 c). The q-ε_q response in Figure 3 b also clearly demonstrates triggering of cyclic instability at point "A". Thus, specimen BC1-14 manifested cyclic instability which triggered at "A".

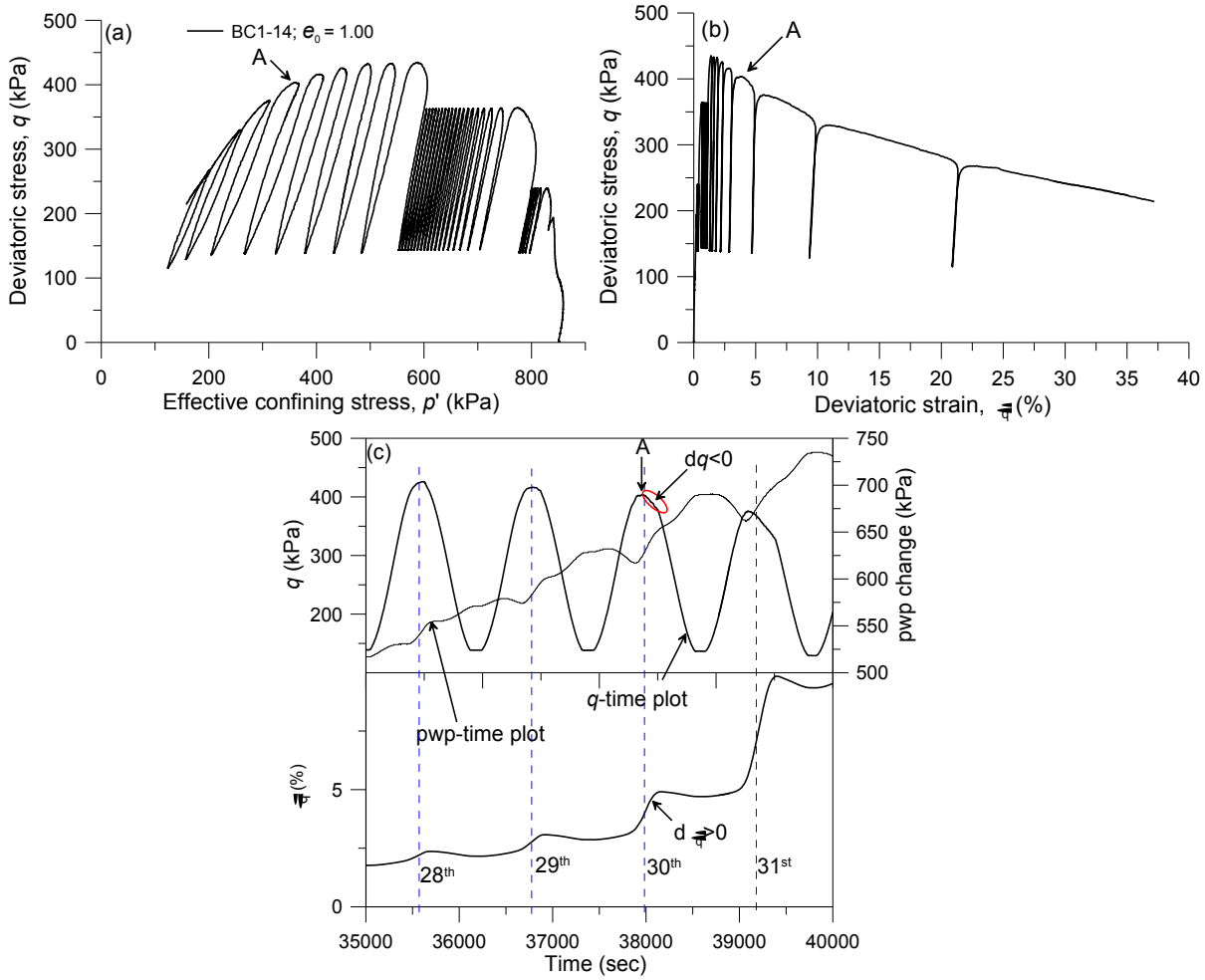

Figure 3. Undrained responses of BC1-14 under one-way cyclic loading showing cyclic instability: (a) ESP, (b) q-ε_q plot and (c) time-trace plots for q, excess pwp & ε_q

4.1.2 Cyclic instability under two-way symmetrical cyclic loading

Test BC2-02 was conducted at p'_0 = 350 kPa with e_0 = 0.99. Its ESP and q-ε_q response are presented in Figures 4 a-b and the time traces of q, excess pwp and ε_q for the few cycles before and after triggering of cyclic instability are in Figure 4 c. "Dotted lines" in the time–trace plots indicate the occurrence (time) of q_{peak} whereas "dashed lines" indicate the occurrence (time) of q_{trough}.

For BC2-02, cyclic loading started with q_{peak} and q_{trough} of 138 kPa and -119 kPa respectively and continued for three loading cycles. After achieving q_{peak} and q_{trough} in the 1st loading cycle, soil specimen failed to do so thereafter. Achieved q_{max} at "B" was less than q_{peak} and cyclic ESP started to plummet downward thereafter (Figure 4 a). At the same time, ε_q increased and thus, satisfied the condition $dq\, d\varepsilon_q < 0$ as a sign of instability (Figures 4 b-c). When the cyclic ESP travelling back to the extension side after point "B", soil liquefied fully as attended minimum deviator stress, q_{min} was only near zero (Figures 4 a-c). A significant loss in soil strength was also observed in the compression side of the last loading cycle while ε_q changed by 28% (Figure 4 c). Thus, this illustration shows that soil specimen BC2-02 manifested cyclic instability which triggered at "B" and after that soil lost its strength almost entirely within one loading cycle.

4.2 Cyclic mobility

Figures 5 a-b show the ESP and q-ε_q response for specimen BC2-07 conducted at p'_0 = 600 kPa with e_0 = 0.82. The time traces of q, excess pwp and ε_q for the few cycles before and after 5% DA ε_q for BC2-07 are plotted in Figure 5 c.

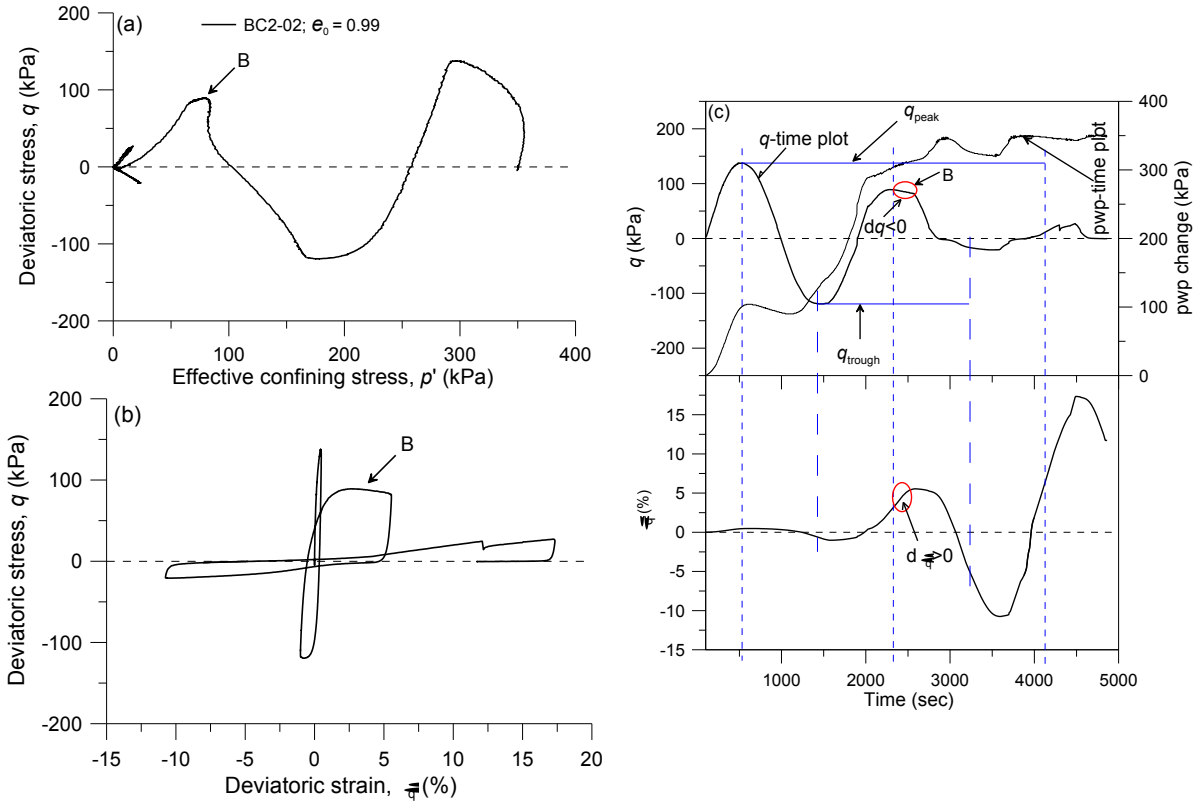

Figure 4. Undrained responses of BC2-02 under two-way symmetrical cyclic loading showing cyclic instability: (a) ESP, (b) q-ε_q plot and (c) time-trace plots for q, excess pwp & ε_q

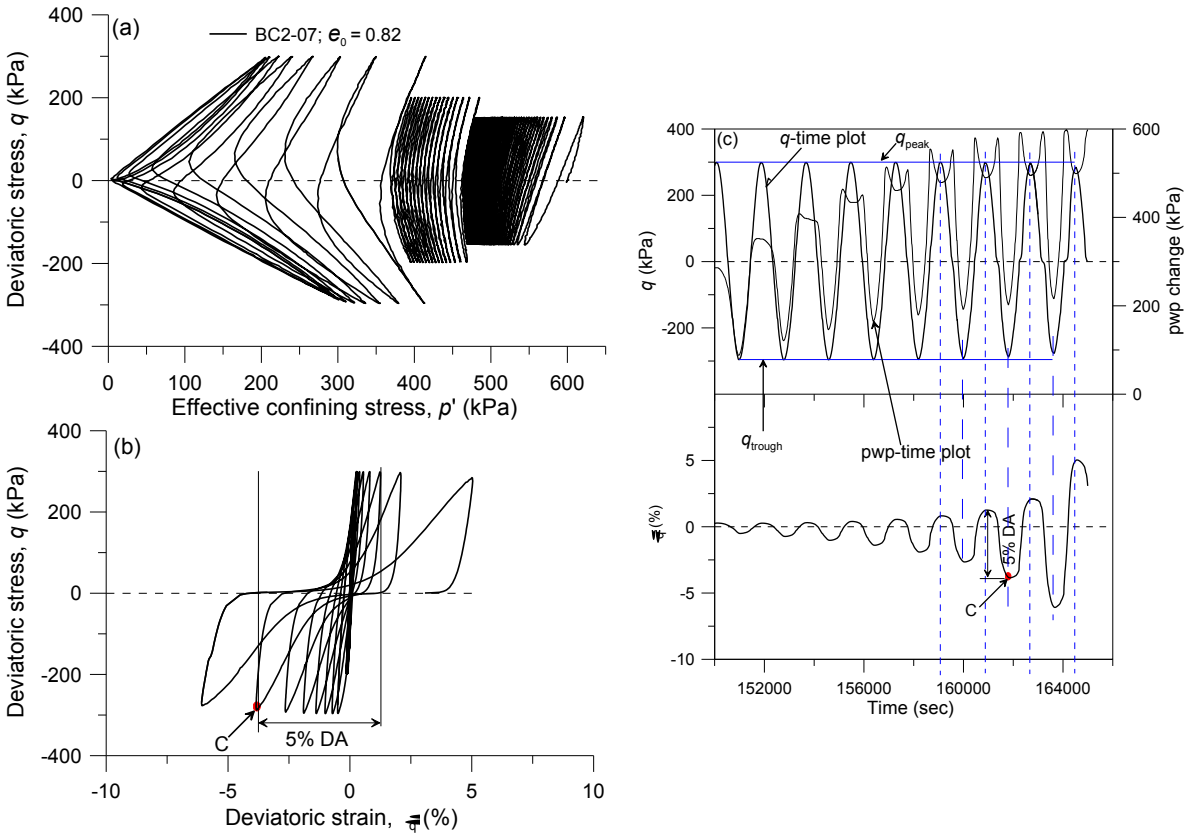

Figure 5. Undrained responses of BC2-07 under two-way symmetrical cyclic loading showing cyclic mobility: (a) ESP, (b) q-ε_q plot and (c) time-trace plots for q, excess pwp & ε_q

Three stages of cyclic loading were imposed for test specimen BC2-07. First stage of loading was continued for 67 cycles with q_{peak} and q_{trough} of 153 kPa and -154 kPa respectively (Figure 5 a). Due to very sloth leftward movement of the cyclic ESP, a second stage of cyclic loading was imposed with changed q_{peak} and q_{trough} of 200 kPa and -198 kPa respectively and continued for another 16 loading cycles. The movement of the cyclic ESP accelerated slightly upon second packet of cyclic loading. At the end of second packet of cyclic loading accumulated maximum ε_q was -0.15% (extension side). To further accelerate the leftward movement of the cyclic ESP, a third stage of cyclic loading was commanded with q_{peak} and q_{trough} of 300 kPa and -296 kPa respectively. Therefore, accelerated leftward movement of the cyclic ESP occurred and brought to near zero transient effective stresses within 7 loading cycles during third stage. Soil accumulated 5% DA ε_q at point "C" (Figure 5 b). It can be seen from Figures 5 a-c that after point "C", soil specimen still could achieve a q_{max} and q_{min} which were nearly same as q_{peak} and q_{trough}. All the sates before and after the point "C", the condition of $dq\,d\varepsilon_q > 0$ was satisfied (Figure 5 c) and thus no sign of instability. Furthermore, there was no abrupt change in excess pwp in the last few cycles before and after the point "C" (Figure 5 c). Moreover, peak and trough points of ε_q and q were matched precisely before and after the point "C" (Figure 5 c). Thus, manifested form of cyclic liquefaction was cyclic mobility.

5 CONCLUSIONS

Different forms of cyclic liquefaction behaviour of coal ash were investigated in this study covering a range of p'_0 = 100 kPa to 850 kPa. The major findings from this study are as follows:

(a) Cyclic instability and cyclic mobility are two distinct forms of cyclic liquefaction and should treat separately while evaluating cyclic strength characteristics of a soil using a certain percentage of DA ε_q criteria.

(b) Within tested range of void ratio, e_0 (0.81-1.08), cyclic instability was manifested for a range of e_0 = 0.96 to 1.08 whereas cyclic mobility was the form of liquefaction for e_0 ranged from 0.81 to 0.85.

(c) After triggering of cyclic instability under one-way cyclic loading (in compression), the coal ash can still developed some residual strength. However, under two-way symmetrical cyclic loading the strength rapidly dropped to very small value.

ACKNOWLEDGEMENTS

The first author was supported by the University College Postgraduate Research Scholarship (UCPRS) during his PhD research on "Cyclic liquefaction behaviour of granular materials with fines" at The University of New South Wales (UNSW), Canberra, Australia. The first author also would like to acknowledge "Research publication fellowship" obtained from the same university.

REFERENCES

Baki, M.A.L., Rahman, M.M., and Lo, S.R. (2011). "Equivalent granular state parameter in predicting different forms of cyclic liquefaction behaviour of sand with fines." Geo-Frontiers 2011, Texas, USA, GSP 211, 1574-1584. doi:10.1061/41165(397)161

Baki, M.A.L., Rahman, M.M., and Lo, S.R. (2012). "Cyclic instability behaviour of coal ash." Geo-Congress 2012, Oakland, USA, GSP 225, pp. 849-858.

Boominathan, A., and Hari, S. (2002). "Liquefaction strength of fly ash reinforced with randomly distributed fibers." Soil Dynamics and Earthquake Engineering, 22 (9-12), 1027-1033.

Ishihara, K. (1993). "Liquefaction and flow failure during earthquakes." Géotechnique, 43 (3), 351-415.

Jakka, R.S., Datta, M., and Ramana, G.V. (2010). "Liquefaction behaviour of loose and compacted pond ash." Soil Dynamics and Earthquake Engineering, 30(7), 580-590.

Lade, P.V. (1994). "Instability and liquefaction of granular materials." Computers and Geotechnics, 16 (2), 123-151.

Lo, S.R., Chu, J., and Lee, I.K. (1989). "A technique for reducing membrane penetration and bedding errors." Geotechnical Testing Journal, 12 (4), 311-316.

Lo, S.R., Rahman, M.M., and Bobei, D.C. (2010). "Limited flow characteristics of sand with fines under cyclic loading." Geomechanics and Geoengineering, 5 (1), 15-25.

Mohamad, R., and Dobry, R. 1986. Undrained monotonic and cyclic triaxial strength of sand. Journal of Geotechnical Engineering, 112 (10): 941-958.

Mohanty, B., Patra, N.R., and Chandra, S. (2010). "Cyclic triaxial behavior of pond ash." GeoFlorida 2010, Florida, USA, GSP 199, 833-841.

Vaid, Y.P., and Sivathayalan, S. (2000). "Fundamental factors affecting liquefaction susceptibility of sands." Canadian Geotechnical Journal, 37 (3), 592-606.